

Fatigue crack tip plastic zones in low carbon steel

D. L. DAVIDSON and J. LANKFORD

Southwest Research Institute, San Antonio, Texas 78284, USA

T. YOKOBORI and K. SATO

Tohoku University, Sendai, Japan

(Received August 8, 1975; in revised form December 19, 1975)

ABSTRACT

Microscopic plastic zone parameters at the tips of fatigue cracks in low carbon steel, as derived by the X-ray microbeam technique, have been correlated with measurement of some of the same parameters by the electron channeling contrast technique. Good correlation has been obtained for the parameters common to both techniques. The results for low carbon steel are found to correlate well with fatigue crack plasticity in other metals.

1. Introduction

Regions of plastic deformation at the tips of fatigue cracks in low carbon steel have been studied extensively by the X-ray microbeam (XMB) technique, in addition to the usual optical and scanning electron microscope methods [1, 2, 3]. More recently, the techniques of electron channeling contrast (ECC) and selected area electron channeling have been used for the same purpose [4, 5]. In order to further understand fatigue crack propagation and gain confidence in the results gained to date, it was felt that a comparison of these techniques on a set of common specimens would be useful.

Accordingly, specimens previously examined by the X-ray microbeam (XMB) technique were examined using the electron channeling contrast (ECC) technique.

2. Experimental procedure

The specimens examined, and reported on herein, were those used in obtaining the results previously reported in [3]. This reference includes information on the chemical and mechanical characteristics of the material used, its thermal history, and the details of the fatigue tests used to grow the cracks studied. XMB techniques, as well as computational details for the parameters presented were reported previously [1, 2]. Table 1 summarizes the referenced data on these specimens.

TABLE 1

Material: 0.5 C; 0.33 Mn; 0.046 Al; 0.022 S; 0.01 Si; 0.006 P (wt.%)
Upper yield (σ_y): 22.1 kg/mm ² (218 MN/m ²)
Lower yield (σ_{y1}): 20.7 kg/mm ² (204 MN/m ²)
Ultimate: 28.5 kg/mm ² (282 MN/m ²)
Elongation: 55.8%
Specimen: 200 mm × 71 mm × 2.7 mm, center notch 2 mm long
Applied fatigue stresses: 0.8 up to 17.2 kg/mm ² (7.9–170.1 MN/m ²)

Four specimens, each having two cracks grown from the central notch, were examined. Table 2 lists the relevant information for these specimens.

TABLE 2

Specimen No.	Stress kg/mm ² (MN/m ²)	ΔK kg/mm ^{3/2} (MN/m ^{3/2})	K_{max}^* kg/mm ^{3/2} (MN/m ^{3/2})	R^{***}	Half crack length C mm	r_p^{**} (calculated) μm	da/dN $\mu\text{m}/\text{cycle}$
H-4	10.43 ± 5.48 (103 ± 54.1)	22.23 (5.89)	33.1 (10.3)	0.31	1.30	318	0.0015
H-8	10.40 ± 5.60 (103 ± 55.4)	39.52 (12.14)	52.3 (16.2)	0.30	3.40	800	0.014
H-9	9.00 ± 8.20 (89 ± 81.1)	59.87 (18.57)	60 (18.6)	0.04	3.82	980	0.036
H-12	8.97 ± 8.07 (88.7 ± 79.8)	83.87 (26.00)	85 (26.5)	0.05	6.37	2500	0.12

* $K_{max} = \sigma_{max}(\pi C)^{1/2} [\sec(\pi C/w)]^{1/2}$; w = plate width (71 mm).

** Calculated plastic zone size $r_p = 0.17 (K/\sigma_y)^2$, which is Rice's [6] relation derived for plane strain.

*** $R = K_{min}/K_{max}$.

3. Experimental results and discussion

Representative channeling contrast photographs from the specimens examined are shown in Figs. 1–5. In each case, what may be seen are the subgrains formed adjacent to the fatigue crack as it propagates through the material. Subgrain formation, such as that shown, was found to result from 2–3% tensile elongation, in general agreement with the observations of Keh and Weissman [7], who noted the beginning of cells at 3% strain, with completely stable cells forming after about 8% strain. Average subgrain diameter has been measured for Specimen H-12 ($\Delta K = 26 \text{ MN/m}^{3/2}$) and is shown in Fig. 6 as a function of distance from the crack. Data shown are the results of ECC measurements from several places along the wake of the crack. Extrapolation back to the region just adjacent to the crack indicates an average cell size of 1–2 μm , compared to the average grain diameter for the material of about 28 μm . For this same ΔK value, the XMB technique value of subgrain size was about 2.5 μm , measured by a spot size roughly 30 μm across. From Fig. 6, with averaging over a 30 μm diameter, 15 μm distance from the crack gives a value of approximately 3 μm . Thus, the agreement between the XMB and ECC technique results is considered to be excellent. At smaller values of ΔK , subgrain formation,

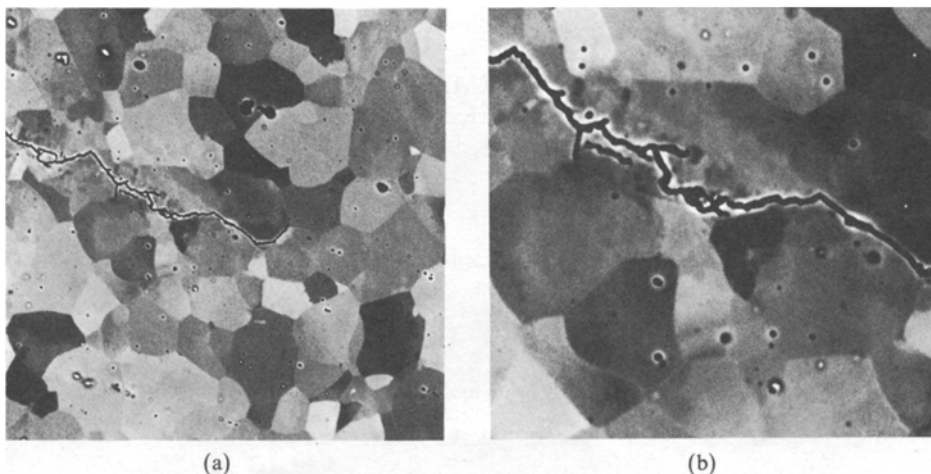


Figure 1. Specimen No. H-4, $\Delta K = 22.23 \text{ kg/mm}^{3/2}$ (5.89 $\text{MN/m}^{3/2}$) showing little distinguishable subgrain formation and a very small plastic zone; (a) 400 \times , (b) 1000 \times .

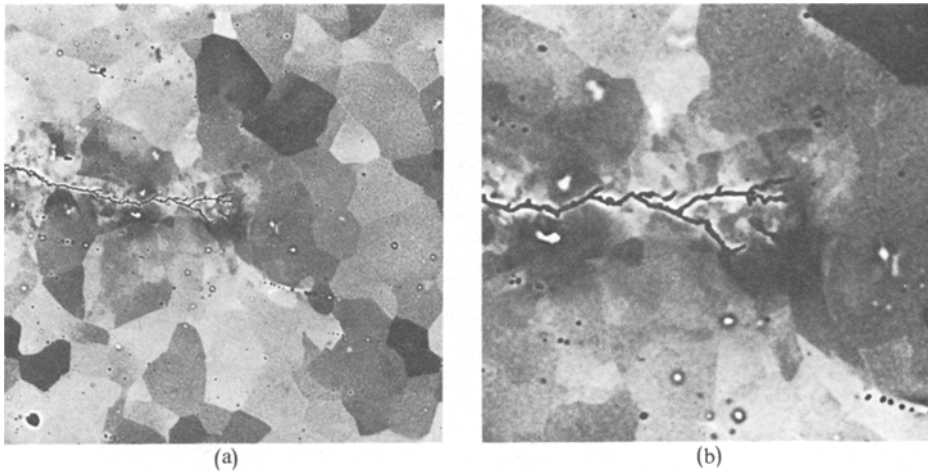


Figure 2. Specimen No. H-8, $\Delta K=39.52 \text{ kg/mm}^{\frac{3}{2}}$ ($12.14 \text{ MN/m}^{\frac{3}{2}}$); (a) $400\times$, (b) $1000\times$.

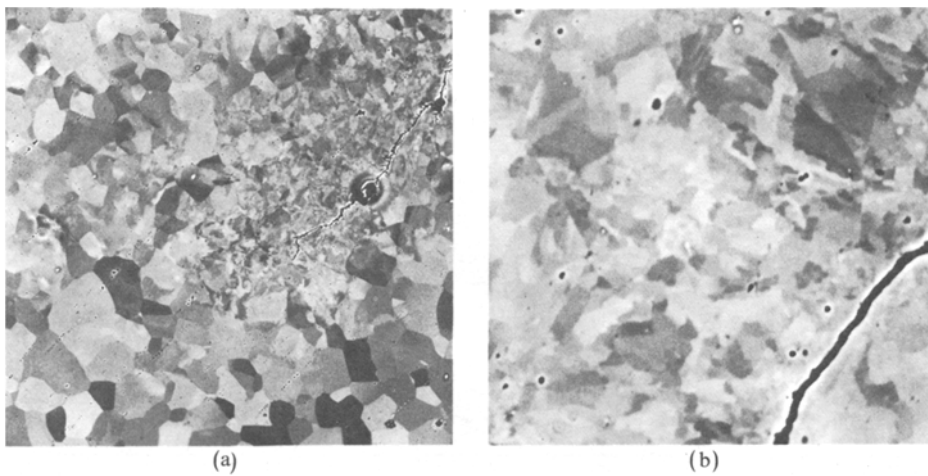


Figure 3. Specimen No. H-9, $\Delta K=59.87 \text{ kg/mm}^{\frac{3}{2}}$ ($18.57 \text{ MN/m}^{\frac{3}{2}}$); (a) and (b) $400\times$.

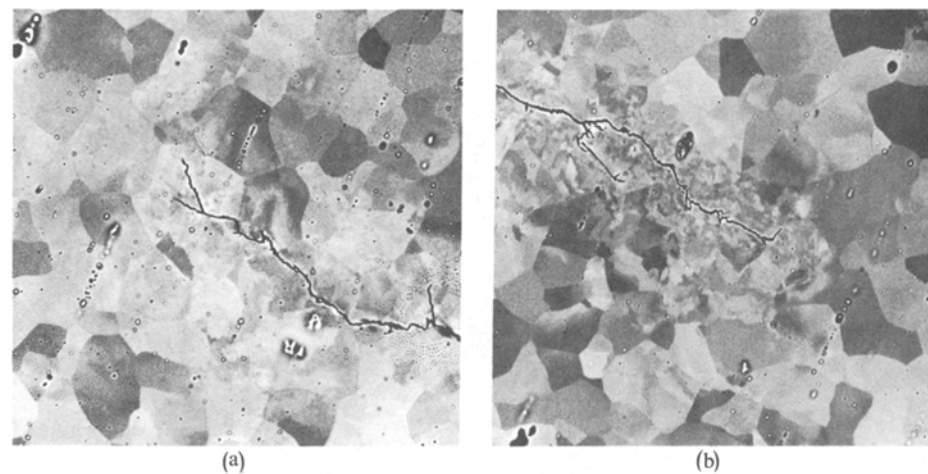


Figure 4. Specimen No. H-12, $\Delta K=83.87 \text{ kg/mm}^{\frac{3}{2}}$ ($26.00 \text{ MN/m}^{\frac{3}{2}}$) showing distinct subgrain formation which has obliterated previous grain boundaries; (a) $400\times$, (b) $1000\times$. Subgrain diameter data shown in Fig. 6.

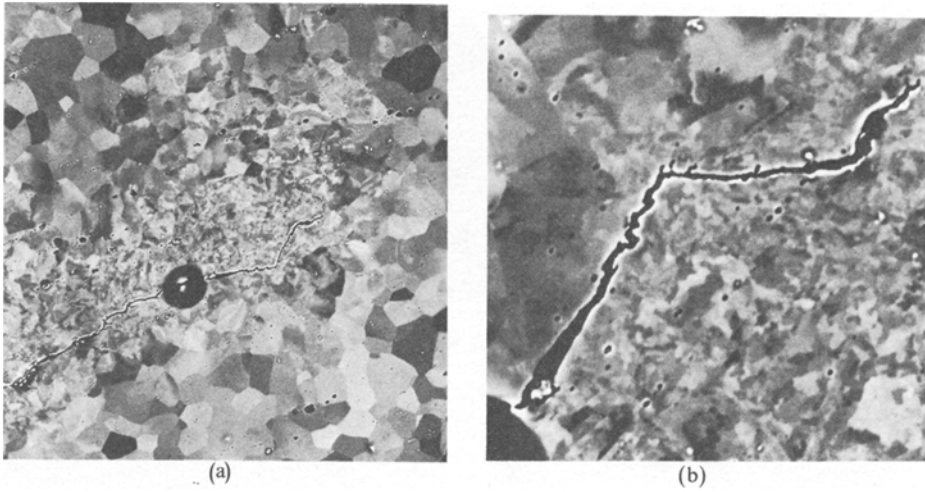


Figure 5. Specimen No. H-12 showing the other of the two cracks seen in Fig. 4; (a) 400 \times , (b) 1000 \times . Subgrain diameter data shown in Fig. 6.

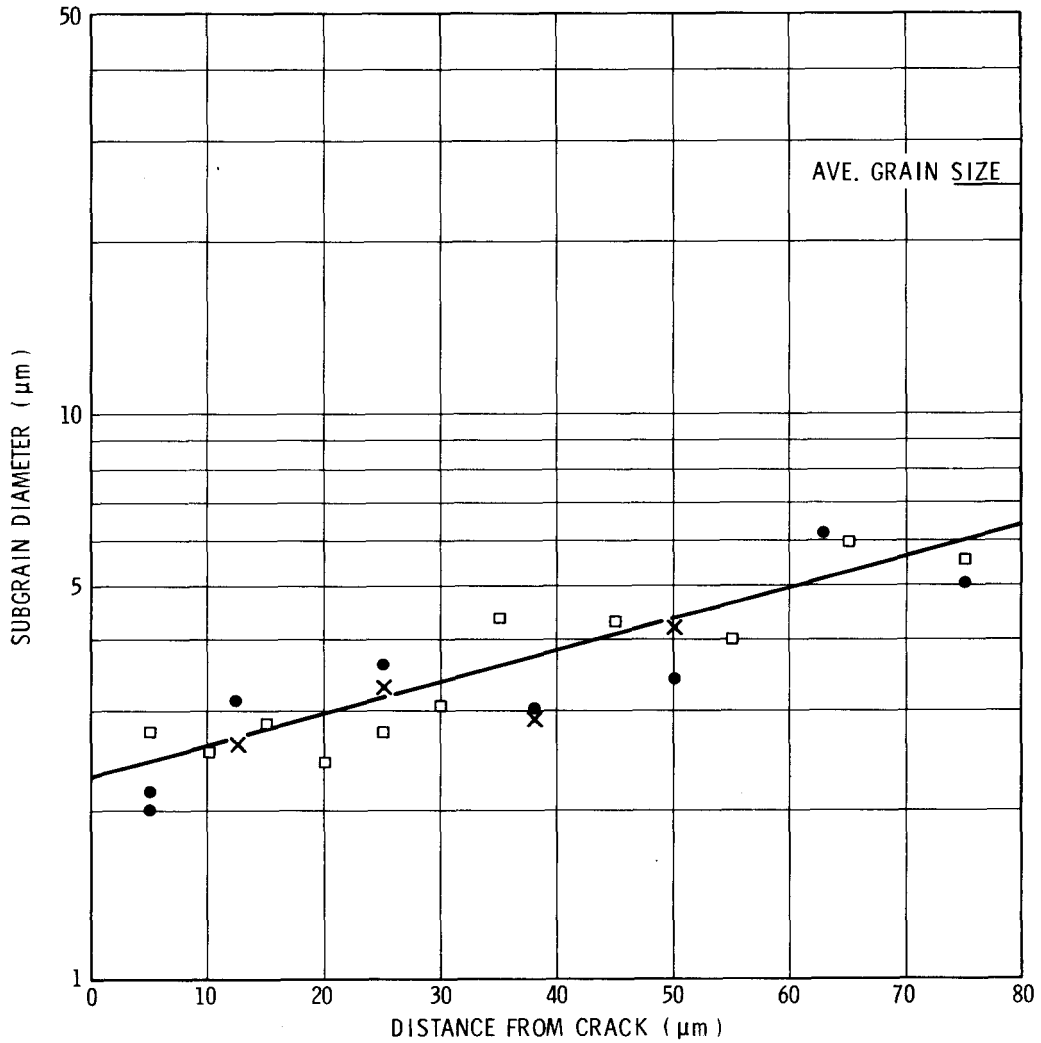


Figure 6. Subgrain size as a function of distance away from the crack. Data taken from Figs. 4b and 5b; different symbols denote separate measurements. $\Delta K = 26 \text{ MN/m}^{3/2}$.

TABLE 3

Specimen No.	ΔK kg/mm ^{3/2} (MN/m ^{3/2})	Dimension of plastic zone		Cell size μm
		to the side mm	ahead mm	
H-4	22.23 (5.89)	0.012-0.02	0	4-6*
H-8	39.52 (12.14)	0.031	0.025	3-5
H-9	59.87 (18.57)	0.05	0.038	2-4
H-12	83.87 (26.00)	0.112	0.09	1-2

* Very poorly defined and inhomogeneous.

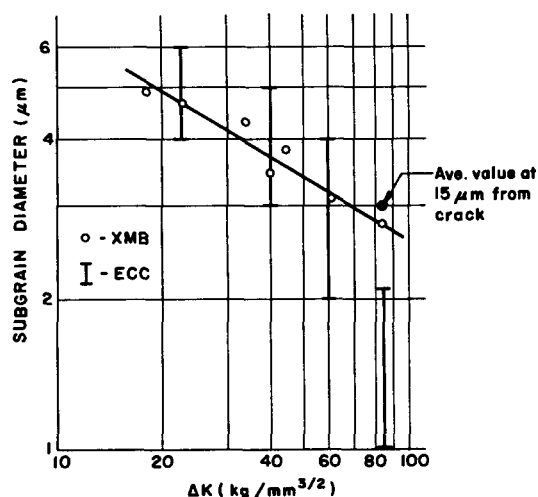


Figure 7. Comparison of subgrain diameters as measured by XMB and ECC correlated with ΔK .

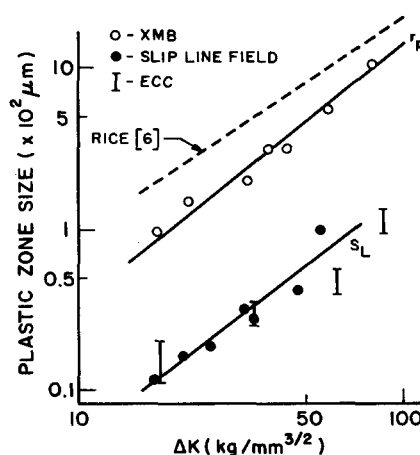


Figure 8. Microscopic plastic zone size as measured by XMB and ECC compared to Rice's calculated size, as compared with ΔK .

as determined by ECC, was found to be highly irregular and inhomogeneous, making direct comparison of results difficult, but the trends are to larger subgrain size, as was previously determined by the XMB studies [3], as well as studies on subgrain formation in pure iron [8] deformed by cyclic loading, Table 3 and Fig. 7.* The subgrain formation seen by the ECC technique is indicative of a dislocation density of 10^9 per sq cm, as determined for both tensile [7] and cyclic [8] deformation. This qualitatively agrees with results of the XMB investigation and with the results of Keh and Weissman [7], who found by TEM minimum cell size of $1.3 \mu\text{m}$ for recrystallized, annealed pure iron deformed to greater than 10% true strain.

Dimensions of the subgrain forming regions adjacent to the fatigue cracks, as determined from ECC measurements, are shown in Table 3. The cell sizes shown were measured as close to the crack as possible (4-8 μm) along the crack wake. As seen in Table 3 and from the ECC photographs, the deformed region is more extensive to the

* The authors are indebted to a reviewer for bringing to their attention the work of Taira [9], who found for 0.03% C annealed steel that XMB examination of fatigue fracture surfaces showed a subgrain size of $1 \mu\text{m}$ to $3 \mu\text{m}$, with the smaller value corresponding to a high crack growth rate, and the latter value corresponding to a low stress intensity, in agreement with Table 3.

side of the crack than directly ahead of it. The measured surface slip band zone, S_L , correlates well with the plastic zone found by ECC observations, Figure 8. Note that the dimension of the outer plastic zone, r_p , is a factor of 7.5 times that of this inner zone; the latter probably corresponds to the reverse-flow cyclic zone proposed by Rice [6]. The slight size difference between the slip band zone and the ECC zone probably exists because the slip band zone was observed on the specimen surface, whereas the ECC observations were made after removal of approximately 0.5 mm of material. The calculated [6] values of r_p are nearly equivalent to those measured by XMB and a factor of 7.5 larger than the plastic zone observed by channeling contrast and slip lines because the plastic zone boundary related to Rice's calculations corresponds to a σ_y for a plastic strain of 0.02%, whereas the ECC measured boundary corresponds to 2–3% plastic strain. It should be noted that based on the original, simple model of Rice, the ratio of r_p to the inner cyclic zone should be 4; in the present case the ratio is found to be ≤ 7.5 . There exist other reported measurements of this factor in agreement with both the latter value [4], as well as the former [10]. This effect should be greater at smaller ΔK values, as it is found to be. Selected area electron channeling patterns could be taken to find the boundary of about $\frac{1}{2}\%$ strain, which would increase the size of the plastic zone and undoubtedly allow better correlation with the theory [4].

TABLE 4

Specimen No.	ΔK kg/mm ^{3/2} (MN/m ^{3/2})	Measured da/dN $\mu\text{m}/\text{cycle}$	Calculated CTOD* μm	Measured subgrain diameter μm
H-4	22.23 (5.89)	0.0015	0.1	4–6
H-8	39.52 (12.14)	0.014	0.4	3–5
H-9	59.87 (18.57)	0.036	1.0	2–4
H-12	83.87 (26.00)	0.12	1.9	1–2

* CTOD (cyclic) = $0.112 (\Delta K)^2 / \sigma_y E$ ([6]) where E = Young's modulus.

Crack growth data do not correlate well with calculated crack tip opening displacements (CTOD). Neither of these quantities appears to be related to subgrain diameter, Table 4. Since the surface of this material was seen to microcrack ahead of the main crack front [3], this result is not totally unexpected; however, no advance microcracking was found using ECC on the interior of the specimen, which leaves unresolved the general occurrence of advance microcracking and its effect on crack growth rate and CTOD. The electron channeling results for the low carbon steel investigated here agree well with those on materials previously investigated (304 SS and Fe-3Si) [4]. Subgrain diameters as a function of distance from the crack for the steel [$(\Delta K/\sigma_y)^2 = 14.5 \text{ mm}$] generally agree with those for 304 SS [$(\Delta K/\sigma_y)^2 = 12.5 \text{ mm}$] even though the material characteristics differ considerably.

The observation of minimum cell sizes (1–2 μm) formed during both cyclic and non-cyclic deformation of iron and steel (bcc) is clearly different from the minimum cell sizes (0.1–0.5 μm) formed during the deformation of copper and aluminium (fcc) [10,11]. The reason for this striking difference is not known.

4. Summary and conclusions

(1) Subgrains formed by the propagation of a fatigue crack may be seen by electron channeling contrast and are found to be of the same size as determined by the X-ray microbeam technique. Subgrains were found to form at approximately 2–3% tensile elongation, which correlates well with results from transmission electron microscopy [7].

(2) Subgrain diameters as measured by both techniques correlate well for all values of cyclic stress intensity.

(3) Plastic zone size as determined by electron channeling contrast measurements is equivalent in size to the observed slip line field. Both these measurements are 0.135 times the size of the outer plastic zone as measured by the X-ray microbeam technique and are thought to coincide with the “inner cyclic plastic zone” concept [6].

REFERENCES

- [1] T. Yokobori, K. Sato and Y. Yamaguchi, *Rep. Res. Inst. Str. Fract. Mat.*, Tohoku Univ., Sendai, Japan, 6 (1970) 49–67.
- [2] T. Yokobori and K. Sato, *Ibid.* 8 (1972) 43–53.
- [3] T. Yokobori, K. Sato and H. Yaguchi, *Ibid.* 9 (1973) 1–10.
- [4] D. L. Davidson and J. Lankford, *Transactions ASME Journal Engineering Materials and Technology*, 98 (1975) 24–29.
- [5] J. Lankford and D. L. Davidson, *Ibid.* 98 (1975) 17–23.
- [6] J. R. Rice, *Fatigue Crack Propagation ASTM STP 415*, American Society Testing Materials (1967) 247.
- [7] A. S. Keh and S. Weissman in *Electron Microscopy and Strength of Crystals*, ed. by G. Thomas and J. Washborn, Interscience (1963) 231.
- [8] F. V. Lawrence, Jr. and R. C. Jones, *Met. Transactions* 1 (1970) 367–393.
- [9] S. Taira and K. Tanaka in *Mechanical Behavior of Materials*, The Society of Materials Science, Japan, II (1972) 48.
- [10] A. Saxena and S. D. Antolovich, *Met. Transactions* 6A, (1975) 1809.
- [11] C. Grosskreutz, *Phys. Stat. Sol. (b)* 47 (1971) 359.

RÉSUMÉ

On met en corrélation les paramètres de la microdéformation plastique à l'extrémité des fissures de fatigue dans l'acier doux, tels qu'ils se déduisent d'une technique de microbombardement par des rayons X, et la mesure de certains de ces paramètres par une technique d'émission électronique à contraste renforcé.

Une bonne corrélation a été obtenue pour les paramètres qui sont communs aux deux techniques et les résultats pour l'acier doux sont en corrélation satisfaisante avec les caractéristiques de plasticité des fissures de fatigue dans d'autres métaux.